Applied Surface Science 439 (2018) 60–65

Contents lists available at ScienceDirect

Applied Surface Science

journal homepage: www.elsevier.com/locate/apsusc

Full Length Article

Mechanical properties of nanodiamond-reinforced hydroxyapatite composite coatings deposited by suspension plasma spraying

Xiuyong Chen [a,*], Botao Zhang [b], Yongfeng Gong [a], Ping Zhou [a], Hua Li [a,*]

[a] Key Laboratory of Marine Materials and Related Technologies, Key Laboratory of Marine Materials and Protective Technologies of Zhejiang Province, Ningbo Institute of Materials Technology and Engineering, Chinese Academy of Sciences, Ningbo 315201, China

[b] Cixi Institute of Biomedical Engineering, Institute of Materials Technology and Engineering, Chinese Academy of Sciences, Ningbo 315201, China

ARTICLE INFO

Article history:
Received 15 September 2017
Revised 12 December 2017
Accepted 2 January 2018
Available online 8 January 2018

Keywords:
Hydroxyapatite
Nanodiamond
Microstructure
Mechanical properties
Suspension plasma spray

ABSTRACT

Hydroxyapatite (HA) coatings suffer from poor mechanical properties, which can be enhanced via incorporation of secondary bioinert reinforcement material. Nanodiamond (ND) possesses excellent mechanical properties to play the role as reinforcement for improving the mechanical properties of brittle HA bioceramic coatings. The major persistent challenge yet is the development of proper deposition techniques for fabricating the ND reinforced HA coatings. In this study, we present a novel deposition approach by plasma spraying the mixtures of ND suspension and micron-sized HA powder feedstock. The effect of ND reinforcement on the microstructure and the mechanical properties of the coatings such as hardness, adhesive strength and friction coefficient were examined. The results showed that the ND-reinforced HA coatings display lower porosity, fewer unmelted particles and uniform microstructure, in turn leading to significantly enhanced mechanical properties. The study presented a promising approach to fabricate ND-reinforced HA composite coatings on metal-based medical implants for potential clinical application.

1. Introduction

Hydroxyapatite (HA) has been widely used in orthopedics, maxillofacial surgery and dental implants due to its excellent biocompatibility and osseointegration in body environment [1–3]. The chemical structure (Ca/P ratio) of HA is very close to human bones and teeth, which makes it bioactive and biocompatible [4]. One of the main applications of HA is that as coatings deposited on bioinert metallic medical implants. Many coating techniques are used to deposit the HA coatings on the surface of metallic implants including sol-gel [5,6], sputtering [7,8], pulsed laser deposition [9,10], and thermal spraying [11,12]. But plasma spray is the only process which has been approved by Food and Drug Administration (FDA) for biomedical coatings due to its good coating properties as compared to other coating processes [13]. However, it has been found that HA coatings suffer mechanical failures such as fracture toughness, hardness, abrasive wear, and bonding strength [11,14,15]. The mechanical stability of HA coatings on titanium alloy substrates has been concerned for long-term clinical application.

To overcome the poor mechanical of HA coatings, bioinert materials with better mechanical properties are used for reinforcement. Previously many researchers suggested that the mechanical properties of HA coatings could be significantly improved by the incorporation of second phases such as yttria stabilized zirconium oxide [16], titanium oxide [17], aluminum oxide [14] and carbon nanotubes (CNTs) [4]. However, few materials that have been considered for HA based composites satisfy both favorable biocompatibility and sufficient mechanical properties. As an alternative novel material, nanodiamond (ND) particles have been attracting intense attentions owing to their unique properties including superior hardness, high thermal conductivity, low friction coefficient, chemical stability and resistance to harsh environments [18]. Moreover, recent reports of the biological performances of ND [19–22] further imply the possibility of ND used as additives in HA coatings for load bearing biomedical applications. However, conventional atmospheric plasma spraying technique typically has high processing temperature which is not conducive to maintaining intact physical and chemical properties of ND powder. Thus, apart from searching a suitable second phase, there is also an urgent need to find a coating preparation technique to meet these requirements. Suspension plasma spray is a relatively new coating deposition technique that uses a feedstock in a form of suspension instead of dry powder and therefore it is of particular prospect for depositing nanosized particles [23–25].

* Corresponding authors.
E-mail addresses: chenxiuyong@nimte.ac.cn (X. Chen), lihua@nimte.ac.cn (H. Li).

https://doi.org/10.1016/j.apsusc.2018.01.014
0169-4332/

In this study, we report novel ND-reinforced HA composite coatings deposited by plasma spraying the mixtures of suspension and powder feedstock. Different from conventional suspension plasma spraying processes, the micron-sized powders and ND contained suspension were fed into the flame separately. The chemical composition and microstructure formation of the HA and ND reinforced HA coatings were investigated. To elucidate the mechanical performances of the coatings, hardness, adhesive strength and frictional tests were carried out. This study provides a competitive approach for processing HA based biomedical materials.

2. Experimental setup

HA powder in nanosize was synthesized via a wet chemical reaction between $(NH_4)_2HPO_4$, $Ca(NO_3)_2$ and NH_3H_2O according to an established protocol [26]. The as-synthesized nanosizes HA powder was poured into 3.0 wt.% polyvinyl alcohol (PVA, as a binder). The HA powder was then mechanically stirred for 5 h to form the slurry and dried at 120 °C. Particle size was given by the manufacturer as 120–400 mesh. For nanodiamond (ND) suspension preparation, ND powders (Qinghai Microcrystalline Nano Technology Co., China) with particle size of ~5 nm were added to the solvent (mixture of distilled water and ethanol with the ratio of 1:1). The suspensions with ND concentration of 0.5 wt.% and 2.0 wt.% were investigated.

HA coatings with/without reinforcement of ND were deposited onto titanium substrates by an APS-2000 K plasma spray system (AVIC Beijing Aeronautical Manufacturing Technology Research Institute, China). The suspension plasma spray system is schematically depicted in Fig. 1d. The spray distances of 100 mm (from the HA powder injector to the substrate) and 50 mm (from the ND suspension injector to the substrate) were adopted for coating deposition. Prior to the spraying, the substrates were surface grit blasted. For plasma spraying, the plasma power is 25 kW. In this study, three different types of coating samples were investigated. They are the HA coating-made from sole HA, the HA/0.5ND coating made from mixture of suspension with ND concentration of 0.5 wt.% and HA powder feedstock and the HA/2.0ND coating-made from mixture of suspension with ND concentration of 2.0 wt.% and HA powder feedstock.

Transmission electron microscopy (TEM, Tecnai F20, USA) and field emission scanning electron microscopy (FEI Quanta FEG250, the Netherlands) were employed for microstructural characterization of the powder and coatings. Raman spectra of the samples were obtained by an inVia Raman Microspectrometer from Renishaw (UK) using 325 nm HeCd laser with a resolution of 1 cm^{-1}. Chemical compositions of the samples were detected by X-ray diffraction (XRD, Bruker AXS, Germany) at a scanning rate of 0.1°/s using Cu Kα radiation operated at 40 kV. Adhesive strength of the HA and HA/ND coatings on titanium substrates were determined by scratch test using a micro-scratch tester (WS-2006, Kaihua Science and Technology Co. Ltd., China). Vickers microhardness of the coatings was determined by Micro-Vickers microhardness tester (HV-1000, Shanghai Lianer Testing Equipment Corporation, China) on polished coatings under a load of 200 g for 10 s. An average microhardness was collected from 5 indents for each sample. The scratches were linear with progressively increasing load. The test was carried out using an initial load of 1.0 N and a final load of 60 N. The increase rate of the load was 12 N/min. Scratch length of 5 mm was employed. The friction signals were used for the estimation of the critical load, Lc. Microtribological properties of HA and HA/ND coatings were studied on a UMT-3MT tribometer (CETR, USA) in reciprocating-sliding mode. Commercially available stainless steel balls (Φ = 3 mm) were used. All the frictional tests were carried out in PBS solution under a load

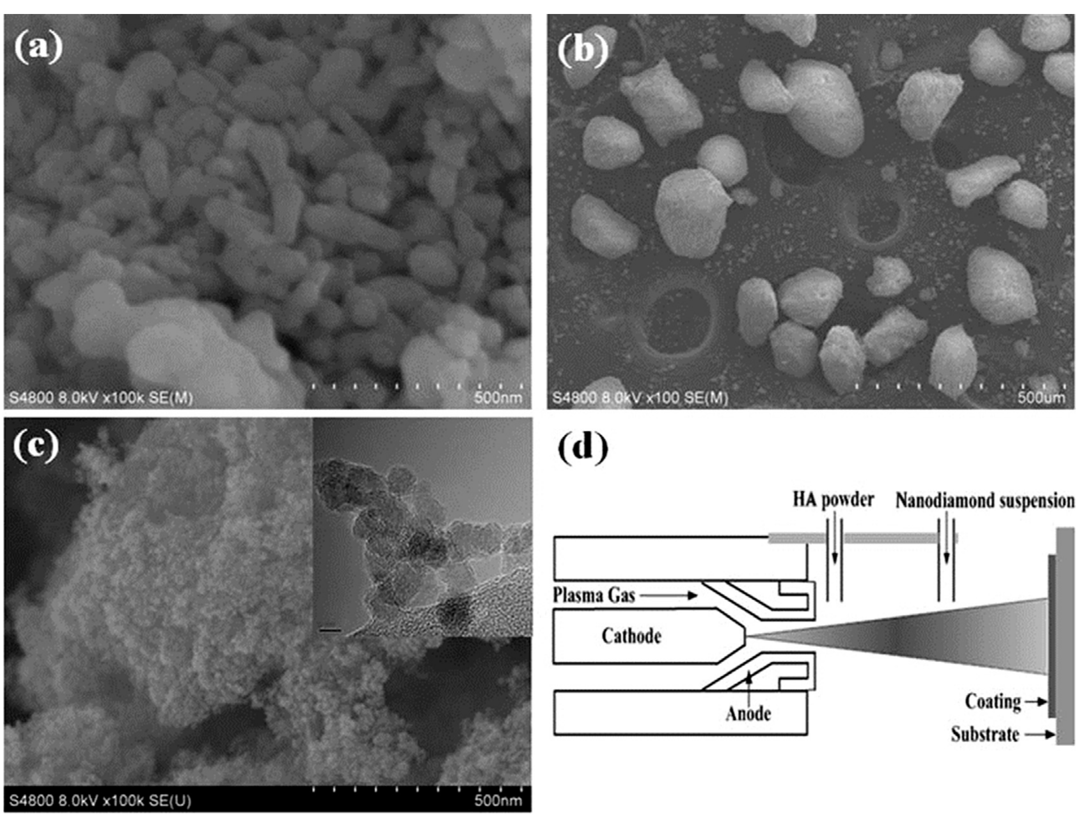

Fig. 1. FE-SEM images of (a) the as-synthesized nanosized HA and (b) the micron-sized HA powder, (c) FE-SEM and TEM images of the as-received ND, and (d) schematic diagram of the suspension plasma spray process.

of 2 N at a constant sliding velocity of 10 mm/s for 60 min. The friction coefficient-time plots were recorded automatically and each measurement was performed three times. The statistical analysis was carried out with OriginPro (version 7.5) at confidence levels of 95, 99.5 and 99.9%.

3. Results and discussion

3.1. Characterization of the powders and coatings

The as-synthesized HA shows a rod-like shape for the HA nanoparticles (Fig. 1a). HA grains have the size of ~20 to 45 nm in length and 10 nm in diameter. The SEM image of the HA micro- powders indicates that the particles have the size of ~75 to 150 μm (Fig. 1b). The as-received ND particles show a primary size of ~5 nm in diameter (Fig. 1c). The aggregation could be clearly seen due to the unstable nature of detonation ND, which agrees well with previous findings [27,28]. Further TEM characterization confirms the aggregation and the (1 1 1) planes of the ND in Fig. 1(c, the inset), which demonstrated that the particle was diamond. Fig. 1d shows the scheme of the deposition of the HA-based nanocomposites on titanium substrates. HA/ND composite coatings were fabricated via a suspension plasma spray approach. The specially designed feeding system favors better protection of ND from flame and easy formation of HA/ND composite coatings.

Fig. 2 presents the scanning electron micrographs of the HA coatings with and without ND reinforcement on titanium substrates. Many particles remained unmelted or partially melted which indicates that the power of 25 kW could not provide sufficient energy to melt all particles and resulted in a non-uniform microstructure in the HA coatings (Fig. 2a-1). The coating shows typical hybrid micro-/nano-structures on its surface due to the decomposition of HA in the hot plasma jet during the spraying process (Fig. 2a-2). The thickness of HA coating is ~30 μm (Fig. 2a-3). When added with 0.5 wt.% ND (Fig. 2b-1), more particles were completely melted and well-flattened particles were deposited. Porosity of the ND reinforced HA coating (~11%) was observed to be much lower than that of pure HA coating (~49%), which is expected since more unmelted or partially melted particles usually results in higher porosity. Similar observation was reported by Yugeswaran et al. for yttria stabilized zirconia reinforced hydroxyapatite coatings [15] and by Singh et al. for Al_2O_3 reinforced hydroxyapatite coatings [29]. Almost all of the HA powder were well melted with 2.0 wt.% ND addition (Fig. 2c-1). In addition, the size of nanostructures on its surface increases with ND content (Fig. 2c-2 vs a-2). The relative density of the HA/ND composite coating increased with adding of ND (Fig. 2b, c). It should be noted here that ND has a thermal conductivity more than 1000 times higher than that of HA [30,31]. Hence it might allow lower cooling rate to the neighboring HA particles, resulting in enhanced melting of HA in the HA/ND composites coating. Moreover, it can be seen that the coating which is far from the substrate displays relative lower density than that next to the substrate (Fig. 2b-3, c-3), which can be explained that the cooling time for molten HA particles also depends on the thermal conductivity of substrate material and thickness of the previously deposited coating.

Besides microstructural effects, the coating stability is largely dependent on the chemical composition and crystallinity of the coatings. X-ray diffraction (XRD) patterns for feedstock and coatings are shown in Fig. 3. The HA feedstock structure (Fig. 3a) is

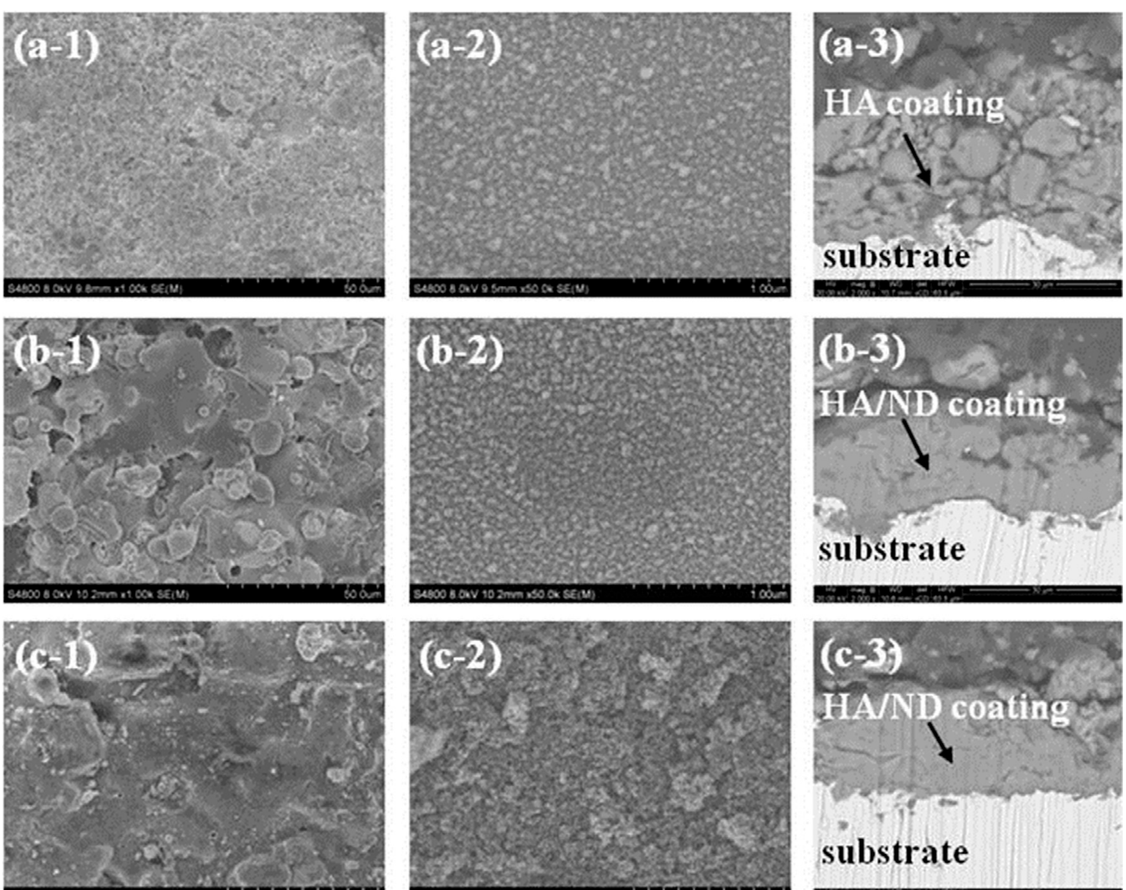

Fig. 2. FE-SEM images of (a) the as-sprayed HA coating, (b) the HA/0.5ND coating, and (c) the HA/2.0ND coating. (−2 is enlarged view of selected area in −1, −3 is cross-sectional view of the coating).

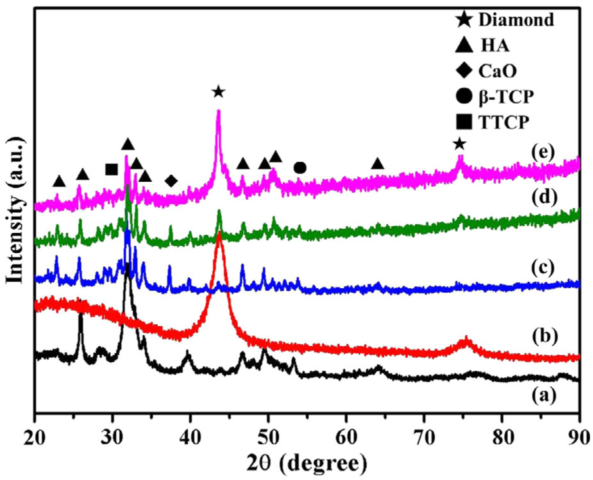

Fig. 3. X-ray diffraction curves of (a) the starting HA powder, (b) the as-received ND powder, and (c) the as-sprayed HA coating, (d) the HA/0.5ND coating and (e) the HA/2.0ND coating.

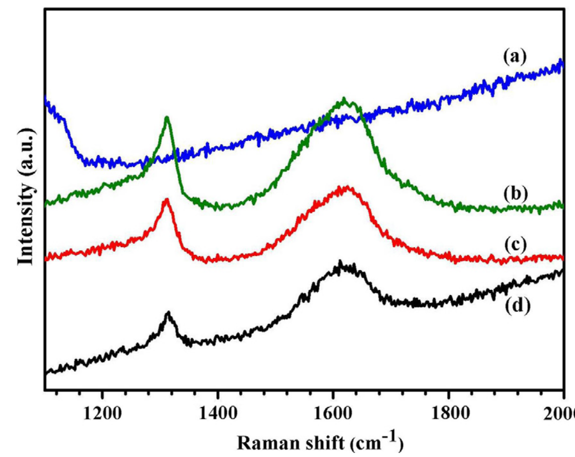

Fig. 4. Raman spectra (325 nm excitation) of (a) the as-sprayed HA coating, (b) the as-received ND powder, (c) the HA/0.5ND coating and (d) the HA/2.0ND coating.

mainly consisted of HA phases (JCPDS card No.: 9-432) [32]. The XRD pattern of the as-received ND particles has two peaks (Fig. 3b) which correspond to the (1 1 1) and (2 2 0) atomic planes of diamond, respectively (JCPDS card No.: 79-1467) [33,34]. The as-sprayed HA and HA/ND composite coatings, apart from the crystalline HA phases, show a small amount of β-tri-calcium phosphate (β-TCP), monoclinic calcium oxide phosphate (TTCP) and calcium oxide (CaO) (Fig. 3c–e). The appearance of β-TCP, TTCP and CaO is related to the decomposition of HA in the hot plasma jet during the spraying process. Similar results have been previously reported during the formation of conventional plasma sprayed HA coatings [14,35,36]. In fact, the existence of small amounts of β-TCP, TTCP and CaO is believed to have no significant effect on the biocompatibility of the HA coatings in physiological environment [37]. It should be noted that ND can be seen between 42° to 44° and 75° to 77° in the XRD patterns of ND-reinforced HA coatings (Fig. 3d, e). The result indicates the successful fabrication of the HA/ND composite coatings with well-retained structure of ND by suspension plasma spray.

To further confirm the successful fabrication of the HA/ND composite coatings with perfectly retained structure of ND, the Raman spectroscopy was used to verify the presence of ND in the composite coatings. Raman spectroscopy is a versatile tool for structural characterization of carbon nanostructures and carbon nanostructure containing composites [38,39]. The as-received ND powders exhibit the characteristic Raman features: the asymmetrically broadened sharp diamond peak around 1325 cm^{-1} and the broad band between 1500 cm^{-1} and 1800 cm^{-1} is assigned to as the "G band" (Fig. 4b), which is consistent with previous studies [18,40]. The HA coating sample does not show any significant Raman signal between 1200–1800 cm^{-1} (Fig. 4a), suggesting that the contribution of HA to Raman signals of the HA/ND composite coatings can be neglected. The Raman spectroscopy curves detected from the surface of the HA/ND composite coatings show well-retained ND, which suggests the efficient protection by suspension plasma spray (Fig. 4c, d). The result further confirmed that the approach proposed here provides an efficient approach for fabricating ND reinforced composite coatings.

3.2. Mechanical performances of the coatings

High hardness is required for a good wear resistance and long service life of metallic implants. The microhardness of coatings increased with an increase in ND content to HA coating (Fig. 5). The HA coating alone has an average HV value of 159. However, the hardness of HA/0.5ND coating and HA/2.0ND coating displayed significantly higher ($p < .05$ and $p < .001$) than that of the HA coating. It can be explained that the ND reinforced HA coatings have much lower porosity as well as high ND content. ND particles can diffuse between HA particles and enhance the hardness of the HA coating. The results are in close agreement with previous studies [40,41]. In addition, the presence of unmelted particles and pores inside the coating microstructure would also play a very important role in the adhesive strength of the coating. Coatings with good mechanical properties could only be obtained from the coatings which has undergone complete melted. Such well-melted HA particles can form maximum contact between the substrate and adjoining layers which would lead to the adhesive and cohesive characteristics needed for the formation of coatings with good mechanical strength. However, the presence of crystalline HA would tend to produce coatings which are porous and mechanically weak in nature due to the limited degree of melting. Therefore, appropriate melting is necessary for the production of coatings with dense microstructure and good mechanical properties. The adhesive strength of the HA coatings as a function of reinforced ND content is also shown in Fig. 5. The result shows that there is a slight improvement in adhesive strength with 0.5% ND

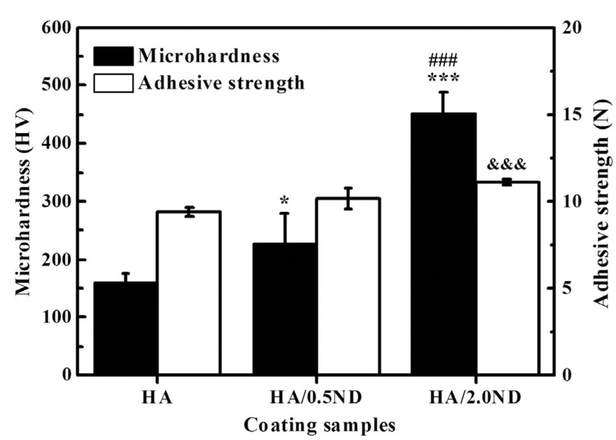

Fig. 5. Vickers hardness and adhesive strength (represented by Lc) of the HA coating and ND reinforced HA coatings. Error bars represent mean ± SD for n = 3. Microhardness: $^{*}p < .05$ and $^{***}p < .001$ compared with HA coating; $^{\#\#\#}p < .005$ compared with HA/0.5ND coating. Adhesive strength: $^{\&\&\&}p < .001$ compared with HA coating.

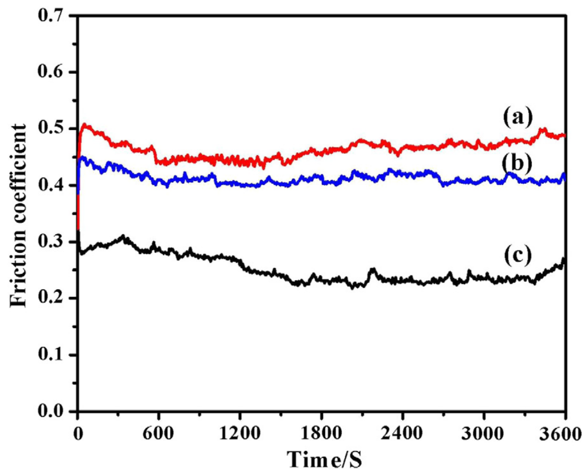

Fig. 6. Variation of friction coefficients with sliding time for HA coatings with/without ND reinforced measured at a load of 2 N: (a) the HA coating, (b) the HA/0.5ND coating, and (c) the HA/2.0ND coating.

reinforcement. Although average higher adhesive strength of HA/0.5ND coating than that of the HA coating, no statistically significant difference was observed between them. It is worth noting that the adhesive strength of HA/2.0ND coating displayed significantly higher ($p < .001$) than that of the HA coating. ND might decrease the cooling rate of the in-flight HA particles thereby causing enhancement of the adhesive strength in HA/ND composite coatings. Similar results were reported that reinforcement of second phase in HA coatings enhanced the bond strength and cohesive strength on titanium substrates [14,16]. Our ongoing efforts are being devoted to clarifying the influence of the reinforcement on the cooling rate of in-flight particles.

The effect of ND reinforcement on the friction coefficient of the HA coatings at 2.0 N load is evaluated in the PBS environment (Fig. 6). The friction coefficient of the pure HA coatings is ∼0.46 (Fig. 6a). The addition of ND results in significant decrease in the friction coefficient (Fig. 6b). The friction coefficient decreases from ∼0.41 for the coating comprising 0.5 wt.% ND to ∼0.25 for the coating comprising 2.0 wt.% ND. This trend might mainly be caused by the reduced porosity and enhanced hardness with respect to ND reinforcement. The result is consistent with the microstructure characterization of the coatings (Fig. 3). Furthermore, the decrease of the friction coefficient might be attributed to ND particles in ND-reinforced HA coatings acting as underprop lubricant with low friction coefficient. Similar results were also reported by Bao et al. for plasma-sprayed Al-Si/nanodiamond composite coatings [42] and by Stravato et al. for HVOF-sprayed nylon-11 + nanodiamond composite coatings [43]. Moreover, carbon nanomaterials, such as fullerenes [44], carbon nanotubes (CNTs) [45,46] and graphene [47,48], have attracted great interest for their demonstrated decreasing friction and increasing wear resistance properties as well as important tribological applications. The result once again confirmed that the HA coating with good mechanical properties was successfully fabricated by ND reinforcement. The novel ND reinforced HA coatings could be potentially used for long service life metallic implants applications.

4. Conclusions

In conclusion, ND-reinforced HA composite coatings were developed on titanium substrates by a suspension plasma spray process. ND structure was well retained in HA/ND composite coatings. The ND-reinforced HA composite coatings displayed lower porosity and uniform microstructure. The mechanical properties of the coatings were significantly enhanced in comparison to pure HA coatings. The approach presented here is potentially important for the development of HA coatings on metal based implants with desirable mechanical properties.

Acknowledgments

This work was supported by National Natural Science Foundation of China (grant # 51401232 and 41706076), Ningbo Municipal Major Projects on Industrial Technology Innovation (grant # 2015B11054), CAS-Iranian Vice Presidency for Science and Technology Joint Research Project (grant # 174433KYSB20160085), International Scientific and Technological Cooperation Project of Ningbo (2017D10011) and Key Research and Development Program of Zhejiang Province (grant # 2017C01003).

References

[1] R.G.T. Geesink, K. Degroot, C. Klein, Bonding of bone to apatite-coated implants, J. Bone Joint Surg. Br. 70 (1988) 17–22.
[2] J.L. Ong, D.C. Chan, Hydroxyapatite and their use as coatings in dental implants: a review, Crit. Rev. Biomed. Eng. 28 (2000) 667–707.
[3] K.E. Salyer, C.D. Hall, Porus hydroxyapatite as an onlay bone-graft substitute for maxillofacial surgery, Plast. Reconstr. Surg. 84 (1989) 236–244.
[4] K. Balani, R. Anderson, T. Laha, M. Andara, J. Tercero, E. Crumpler, A. Agarwal, Plasma-sprayed carbon nanotube reinforced hydroxyapatite coatings and their interaction with human osteoblasts *in vitro*, Biomaterials 28 (2007) 618–624.
[5] P. Choudhury, D.C. Agrawal, Sol-gel derived hydroxyapatite coatings on titanium substrates, Surf. Coat. Technol. 206 (2011) 360–365.
[6] H. Tang, T.Z. Xin, Y. Luo, F.P. Wang, *In vitro* degradation of AZ31 magnesium alloy coated with hydroxyapatite by sol-gel method, Mater. Sci. Technol. 29 (2013) 547–552.
[7] J. Shin, K. Lee, J. Koh, H. Son, H. Kim, H.P. Lim, K. Yun, G. Oh, S. Lee, H. Oh, K. Lee, G. Hwang, S.W. Park, Hydroxyapatite coatings on nanotubular titanium dioxide thin films prepared by radio frequency magnetron sputtering, J. Nanosci. Nanotechnol. 13 (2013) 5807–5810.
[8] M.A. Surmeneva, M.V. Chaikina, V.I. Zaikovskiy, V.F. Pichugin, V. Buck, O. Prymak, M. Epple, R.A. Surmenev, The structure of an RF-magnetron sputter-deposited silicate-containing hydroxyapatite-based coating investigated by high-resolution techniques, Surf. Coat. Technol. 218 (2013) 39–46.
[9] C. Capuccini, P. Torricelli, F. Sima, E. Boanini, C. Ristoscu, B. Bracci, G. Socol, M. Fini, I.N. Mihailescu, A. Bigi, Strontium-substituted hydroxyapatite coatings synthesized by pulsed-laser deposition: *in vitro* osteoblast and osteoclast response, Acta Biomater. 4 (2008) 1885–1893.
[10] H. Khandelwal, G. Singh, K. Agrawal, S. Prakash, R.D. Agarwal, Characterization of hydroxyapatite coating by pulse laser deposition technique on stainless steel 316 L by varying laser energy, Appl. Surf. Sci. 265 (2013) 30–35.
[11] Y.C. Tsui, C. Doyle, T.W. Clyne, Plasma sprayed hydroxyapatite coatings on titanium substrates part 1: mechanical properties and residual stress levels, Biomaterials 19 (1998) 2015–2029.
[12] P.S. Prevey, X-Ray diffraction characterization of crystallinity and phase composition in plasma-sprayed hydroxyapatite coatings, J. Therm. Spray Technol. 9 (2000) 369–376.
[13] K. Balani, Y. Chen, S.P. Harimkar, N.B. Dahotre, A. Agarwal, Tribological behavior of plasma-sprayed carbon nanotube-reinforced hydroxyapatite coating in physiological solution, Acta Biomater. 3 (2007) 944–951.
[14] M. Mittal, S.K. Nath, S. Prakash, Improvement in mechanical properties of plasma sprayed hydroxyapatite coatings by Al_2O_3 reinforcement, Mater. Sci. Eng. C-Mater. 33 (2013) 2838–2845.
[15] S. Yugeswaran, C.P. Yoganand, A. Kobayashi, K.M. Paraskevopoulos, B. Subramanian, Mechanical properties, electrochemical corrosion and *in-vitro* bioactivity of yttria stabilized zirconia reinforced hydroxyapatite coatings prepared by gas tunnel type plasma spraying, J. Mech. Behav. Biomed. 9 (2012) 22–33.
[16] Y.W. Gu, K.A. Khor, D. Pan, P. Cheang, Activity of plasma sprayed yttria stabilized zirconia reinforced hydroxyapatite/Ti-6Al-4V composite coatings in simulated body fluid, Biomaterials 25 (2004) 3177–3185.
[17] X.B. Zheng, C.X. Ding, Characterization of plasma-sprayed hydroxyapatite/TiO_2 composite coatings, J. Therm. Spray Technol. 9 (2000) 520–525.
[18] V.N. Mochalin, O. Shenderova, D. Ho, Y. Gogotsi, The properties and applications of nanodiamonds, Nat. Nanotechnol. 7 (2012) 11–23.
[19] D.Y. Li, X.Y. Chen, Y.F. Gong, B.T. Zhang, Y. Liu, P. Jin, H. Li, Synthesis and vacuum cold spray deposition of biofunctionalized nanodiamond/hydroxyapatite nanocomposite for biomedical applications, Adv. Eng. Mater. (2017), https://doi.org/10.1002/adem.201700363.
[20] V. Vaijayanthimala, P.Y. Cheng, S.H. Yeh, K.K. Liu, C.H. Hsiao, J.I. Chao, H.C. Chang, The long-term stability and biocompatibility of fluorescent nanodiamond as an *in vivo* contrast agent, Biomaterials 33 (2012) 7794–7802.

[21] X. Zhang, S. Wang, M. Liu, J. Hui, B. Yang, L. Tao, Y. Wei, Surfactant-dispersed nanodiamond: biocompatibility evaluation and drug delivery applications, Toxicol. Res. 2 (2013) 335–342.
[22] A.M. Schrand, S.A.C. Hens, O.A. Shenderova, Nanodiamond particles: properties and perspectives for bioapplications, Crit. Rev. Solid State 34 (2009) 18–74.
[23] A. Cattini, L. Łatka, D. Bellucci, G. Bolelli, A. Sola, L. Lusvarghi, L. Pawłowski, V. Cannillo, Suspension plasma sprayed bioactive glass coatings: effects of processing on microstructure, mechanical properties and *in-vitro* behaviour, Surf. Coat. Technol. 220 (2013) 52–59.
[24] O. Marchand, L. Girardot, M.P. Planche, P. Bertrand, Y. Bailly, G. Bertrand, An insight into suspension plasma spray: injection of the suspension and its interaction with the plasma flow, J. Therm. Spray Technol. 20 (2011) 1310–1320.
[25] X.Y. Chen, J.H. Yuan, J. Huang, K. Ren, Y. Liu, S.Y. Lu, H. Li, Large-scale fabrication of superhydrophobic polyurethane/nano-$A_{l2}O_3$ coatings by suspension flame spraying for anti-corrosion applications, Appl. Surf. Sci. 311 (2014) 864–869.
[26] D.Y. Li, Y.F. Gong, X.Y. Chen, B.T. Zhang, H.J. Zhang, P. Jin, H. Li, Room-temperature deposition of hydroxyapatite/antibiotic composite coatings by vacuum cold spraying for antibacterial applications, Surf. Coat. Tech. 330 (2017) 87–91.
[27] M.V. Korobov, D.S. Volkov, N.V. Avramenko, L.A. Belyaeva, P.I. Semenyuk, M.A. Proskurnin, Improving the dispersity of detonation nanodiamond: differential scanning calorimetry as a new method of controlling the aggregation state of nanodiamond powders, Nanoscale 5 (2013) 1529–1536.
[28] A. Kruger, F. Kataoka, M. Ozawa, T. Fujino, Y. Suzuki, A.E. Aleksenskii, A.Y. Vul, E. Osawa, Unusually tight aggregation in detonation nanodiamond: identification and disintegration, Carbon 43 (2005) 1722–1730.
[29] G. Singh, S. Singh, S. Prakash, Surface characterization of plasma sprayed pure and reinforced hydroxyapatite coating on Ti_6Al_4V alloy, Surf. Coat. Technol. 205 (2011) 4814–4820.
[30] D.Y. Kim, Y.H. Han, J.H. Lee, I.K. Kang, B.K. Jang, S. Kim, Characterization of multiwalled carbon nanotube-reinforced hydroxyapatite composites consolidated by spark plasma sintering, Biomed Res. Int. 2014 (2014) 768254.
[31] A.M. Abyzov, S.V. Kidalov, F.M. Shakhov, High thermal conductivity composites consisting of diamond filler with tungsten coating and copper (silver) matrix, J. Mater. Sci. 46 (2011) 1424–1438.
[32] A.P. Kumar, K.K. Mohaideen, S.A.S. Alariqi, R.P. Singh, Preparation and characterization of bioceramic nanocomposites based on Hydroxyapatite (HA) and Carboxymethyl Cellulose (CMC), Macromol. Res. 18 (2010) 1160–1167.
[33] S.P. Gubin, O.V. Popkov, G.Y. Yurkov, V.N. Nikiforov, Y.A. Koksharov, N.K. Eremenko, Magnetic nanoparticles fixed on the surface of detonation nanodiamond microgranules, Diam. Relat. Mater. 16 (2007) 1924–1928.
[34] Y. Liu, Z.N. Gu, J.L. Margrave, V.N. Khabashesku, Functionalization of nanoscale diamond powder: fluoro-, alkyl-, amino-, and amino acid-nanodiamond derivatives, Chem. Mater. 16 (2004) 3924–3930.
[35] S.W.K. Kweh, K.A. Khor, P. Cheang, Plasma-sprayed Hydroxyapatite (HA) coatings with flame-spheroidized feedstock: microstructure and mechanical properties, Biomaterials 21 (2000) 1223–1234.
[36] J.E. Tercero, S. Namin, D. Lahiri, K. Balani, N. Tsoukias, A. Agarwal, Effect of carbon nanotube and aluminum oxide aaddition on plasma-sprayed hydroxyapatite coating's mechanical properties and biocompatibility, Mater. Sci. Eng. C-Mater. 29 (2009) 2195–2202.
[37] Y. Cao, J. Weng, J.Y. Chen, J.M. Feng, Z.J. Yang, X.D. Zhang, Water vapour-treated hydroxyapatite coatings after plasma spraying and their characteristics, Biomaterials 17 (1996) 419–424.
[38] A.C. Ferrari, J. Robertson, Raman spectroscopy of amorphous, nanostructured, diamond-like carbon, and nanodiamond, Philos. T. Roy. Soc. A 362 (2004) 2477–2512.
[39] J.R. Dennison, M. Holtz, G. Swain, Raman spectroscopy of carbon materials, Spectroscopy 11 (1996) 38–46.
[40] D.J. Woo, B. Sneed, F. Peerally, F.C. Heer, L.N. Brewer, J.P. Hooper, S. Osswald, Synthesis of nanodiamond-reinforced aluminum metal composite powders and coatings using high-energy ball milling and cold spray, Carbon 63 (2013) 404–415.
[41] E. Pecheva, L. Pramatarova, T. Hikov, D. Fingarova, Y. Tanaka, H. Sakamoto, H. Doi, Y. Tsutsumi, T. Hanawa, Apatite-nanodiamond composite as a functional coating of stainless steel, Surf. Interface Anal. 42 (2010) 475–480.
[42] M. Bao, C. Zhang, D. Lahiri, A. Agarwal, The Tribological behavior of plasma-sprayed Al-Si composite coatings reinforced with nanodiamond, JOM 64 (2012) 702–708.
[43] A. Stravato, R. Knight, V. Mochalin, S.C. Picardi, HVOF-sprayed nylon-11 +nanodiamond composite coatings: production & characterization, J. Therm. Spray Techn. 17 (2008) 812–817.
[44] B.C. Ku, Y.C. Han, J.E. Lee, J.K. Lee, S.H. Park, Y.J. Hwang, Tribological effects of fullerene (C60) nanoparticles added in mineral lubricants according to its viscosity, Int. J. Precis. Eng. Man. 11 (2010) 607–611.
[45] C. Chen, X. Chen, L. Xu, Z. Yang, W. Li, Modification of multi-walled carbon nanotubes with fatty acid and their tribological properties as lubricant additive, Carbon 43 (2005) 1660–1666.
[46] Z. Xu, Q. Zhang, X. Shi, W. Zhai, Q. Zhu, Comparison of tribological properties of NiAl matrix composites containing graphite, carbon nanotubes, or graphene, J. Mater Eng. Perform. 24 (2015) 1926–1936.
[47] Z. Xu, X. Shi, W. Zhai, J. Yao, S. Song, Q. Zhang, Preparation and tribological properties of TiAl matrix composites reinforced by multilayer graphene, Carbon 67 (2014) 168–177.
[48] P. Hvizdos, Jn Dusza, C. Balazsi, Tribological properties of Si_3N_4/graphene nanocomposites, J. Eur. Ceram. Soc. 33 (2013) 2359–2364.